Applied Physics B (2024) 130:4
https://doi.org/10.1007/s00340-023-08144-2

Applied Physics B
Lasers and Optics

RESEARCH

Sapphire-based resonant waveguide-grating mirrors: advancing their intra-cavity power density capability

Danish Bashir[1] · Ayoub Boubekraoui[1] · Georgia Mourkioti[2] · Fangfang Li[3] · Petri Karvinen[3] · Markku Kuittinen[3] · Jacob. I. Mackenzie[2] · Thomas Graf[1] · Marwan Abdou Ahmed[1]

Received: 28 September 2023 / Accepted: 13 November 2023

Abstract
We report on the design, fabrication, and implementation of a single-layer resonant waveguide-grating (RWG) mirror on a sapphire substrate. Our goal is to enhance these optics capability to withstand high intra-cavity power densities by exploiting the superior thermal properties of sapphire. The RWG was implemented as an intra-cavity folding mirror in an Yb:YAG thin-disk laser to generate linearly polarized and spectrally stabilized radiation. A linearly polarized output power of 191 W with an optical efficiency of 39% was obtained in multi-mode operation. This corresponds to a power density of 52 kW/cm^2 on the RWG, for which the increase of its surface temperature was measured to be 12 K, which resulted in a 46-fold reduction of the surface temperature rise dependence on the intra-cavity power density with respect to what has been reported for a RWG on a fused silica substrate. In near fundamental-mode operation, a linearly polarized emission with an output power of 90 W, an optical efficiency of 30%, and a spectral bandwidth of 28 pm FWHM was obtained.

1 Introduction

Resonant waveguide-gratings (RWGs) provide the possibility to control the polarization and the spectral properties of laser systems [1]. For a specific combination of polarization, wavelength, and angle of incidence (AOI), the resonance leads to an enhanced reflection or transmission [2]. The potential and versatility that RWGs offer has led to their implementation in different applications [3–5] and numerous laser architectures [6–9] and their benefits were also exploited for the demonstration of highly efficient second harmonic generation (515 nm) at an average power exceeding 1 kW [10]. Single-layer RWGs are typically based on sub-wavelength gratings fabricated in a high-index waveguide (such as Ta_2O_5 or Nb_2O_5) deposited on a fused-silica substrate. In this configuration however, they often suffer from significant heating due to the absorption of the radiation in the waveguide layer and the relatively low thermal conductivity of the fused-silica substrate. As such, these devices can only withstand comparably low power densities of about 15 kW/cm^2, limited by the maximum acceptable temperature rise of about 100 K to avoid damage of the component, thus limiting power scaling opportunities [6]. Furthermore, to investigate the damage threshold constraints and how to improve laser performance, a series of experiments were made with a partial reflector, consisting of a varying number of pairs of quarter-wave layers, added to the single-layer RWG [7]. Using this approach for an RWG that was used as a folding mirror in a fundamental-mode Yb:YAG thin-disk laser (TDL), both the laser and the thermal performance of the RWG was improved, allowing a power density of 60 kW/cm^2 on the RWG, at which point the surface temperature rise was 63 K. To further improve the thermal performance of RWGs, we investigate the implementation of a single-layer Ta_2O_5 waveguide layer deposited on a structured sapphire (α-Al_2O_3) substrate. This substrate material is routinely used for highly robust optical components and offers a thermal conductivity exceeding that of fused silica by one order of magnitude. The RWG was intended to be used as an intra-cavity element in an Yb:YAG

Danish Bashir and Ayoub Boubekraoui are contributed equally to this work.

✉ Marwan Abdou Ahmed
marwan.abdou-ahmed@ifsw.uni-stuttgart.de

[1] Institut Für Strahlwerkzeuge, University of Stuttgart, 70569 Stuttgart, Germany

[2] Optoelectronics Research Centre, University of Southampton, Southampton SO17 1BJ, UK

[3] Center for Photonics Sciences, University of Eastern Finland, P.O. Box 111, 80101 Joensuu, Finland

Published online: 07 December 2023

TDL and had the dual tasks of defining a linear polarization and locking the emitted laser wavelength to a narrow spectral bandwidth. As reported below, the results demonstrate the significant influence that the substrate and the grating design has on the thermal stability of the component when exposed to high power densities. The proposed approach clearly reveals the potential to scale the average power even further: as compared to its fused-silica counterpart the sapphire RWG exhibits a 40 times reduced surface temperature rise dependence on the intra-cavity power density.

2 Design

To exploit sapphire's higher thermal conductivity compared with silica, the grating design was optimized to shorten the propagation length,*L*, of the radiation in the waveguide, thus reducing the thermal load due to finite absorption in the Ta_2O_5 film. As described analytically in [11], the propagation length, *L,* is inversely proportional to the grating depth. This is why a structure with a deeper grating than what was reported in [6] has been implemented here. A schematic of the designed device is shown on the left of Fig. 1, comprising a structured sapphire substrate ($n_o = 1.755$ and $n_e = 1.747$ [12] at 1030 nm) on top of which a single layer of Ta_2O_5 ($n = 2.087$) is deposited, acting as the waveguide. The structured substrate was chosen to exploit the double-corrugation effect, effectively shortening the propagation length *L* of the guided radiation [11]. We used a simulation code based on rigorous coupled-wave analysis (RCWA) [13] to find the opto-geometric parameters that lead to a resonance for TE polarized (electric-field parallel to the grating lines) radiation at a wavelength of 1030 nm. The nominal design parameters were a grating period of $\Lambda = 515$ nm, a groove depth of $\sigma = 100$ nm, a duty-cycle of DC = 50% (DC = w/Λ, w being the width of the ridge), and a thickness of the Ta_2O_5 waveguide layer of d = 230 nm. At resonance for an AOI of 11.3°, the calculated reflectance spectra are shown on the right of Fig. 1, for TE and TM polarized radiation with maxima for $R_{TE} = 99.9\%$ and $R_{TM} = 4.5\%$, respectively. The spectral bandwidth of the reflection peak for the TE polarized radiation was 12.6 nm FWHM and 4.1 nm when measured at a height of R = 90%. Both of the above properties, i.e., the difference in the reflectance for TE and TM polarized radiation and the spectral bandwidth of the resonances, ensure the polarization and wavelength selectivity of our device.

3 Fabrication

For the fabrication of the RWG samples, several 10 mm × 10 mm binary gratings spaced by 4 mm were patterned onto a 650 µm thick (0001) sapphire substrate, which had a diameter of 100 mm, using electron-beam lithography. A 50 nm thick chromium (Cr) layer and a 200 nm thick SiO_2 layer were used as etching masks. The pattern was transferred from the electron-beam resist to the Cr layer and then to the SiO_2 layer using inductively coupled plasma (ICP) tools (Oxford Plasmalab 100 and Plasmalab 80). The substrate was then diced into the individual samples measuring 12 mm × 12 mm and etched using another ICP tool (OPT Sys100 ICP380-Plasmalab) [14]. A target thickness of 230 nm of Ta_2O_5 was subsequently deposited on top of two of the structured samples using RF magnetron sputtering (Plasmalab 400 + , Oxford Instruments Plasma Technology) from a dense Tantalum ceramic target.

4 Characterization

In a first step, the wavelength and polarization-dependent reflectance of the fabricated RWGs were measured by means of a setup built according to DIN EN ISO 13697. Similar reflectance was obtained for both samples. Figure 2 shows the measured reflectance at the observed resonance AOI of 11.5°, tuned to obtain the TE peak at the central emission wavelength of 1030 nm of the Yb:YAG TDL. The reflectance for TE and TM polarized radiation was measured to

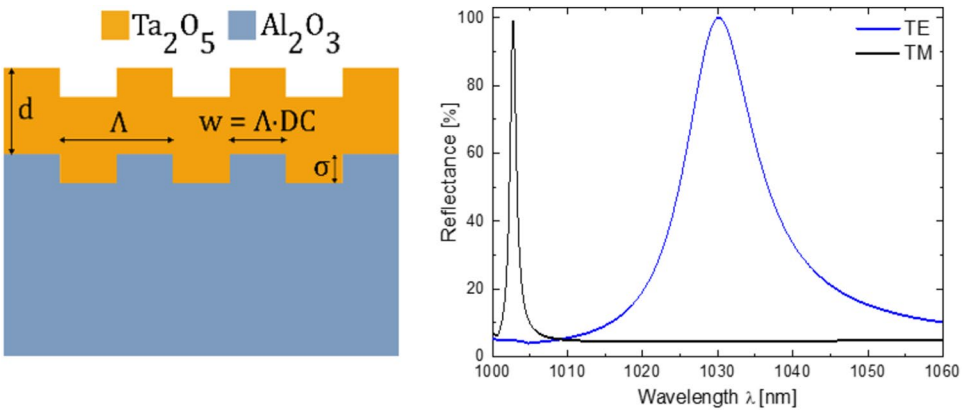

Fig. 1 Left: Schematic of the device. The grating is etched into sapphire with a period of Λ = 515 nm, a groove depth of σ = 100 nm, and a duty-cycle of 50%. A 230 nm-thick layer of Ta_2O_5 is deposited on top of the etched grating. Right: calculated spectral reflectance at an AOI of 11.3° for TE and TM polarized radiation

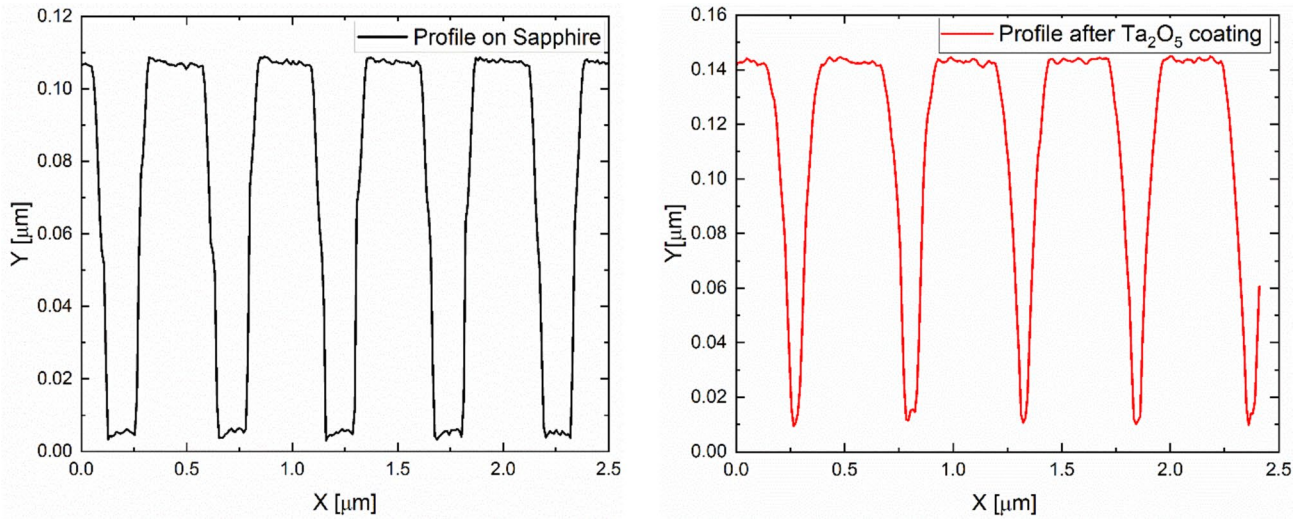

Fig. 2 AFM measurement of grating profiles. Left: AFM scan for the sapphire grating (before Ta_2O_5 coating). Right: AFM scan after deposition of Ta_2O_5 waveguide layer. Note: there is an arbitrary origin in these plots to illustrate the entire profile

be $R_{TE} = 99.2 \pm 0.2\%$ and $R_{TM} = 8 \pm 0.2\%$, respectively. The measured reflectance for TM polarized radiation at 1030 nm was higher than that expected due to Fresnel reflection. This discrepancy is attributed to the fact that the simulation does not consider the reflection at the back surface of the relatively thin substrate. The experimentally determined resonance angle at 11.5° was slightly shifted compared to the design value, which is mainly attributed to the deviation of the opto-geometrical parameters of the grating and waveguide. As shown in Fig. 2, Atomic Force Microscope (AFM) measurements performed on the sample before Ta_2O_5 coating, revealed a trapezoidal sapphire grating profile with a side wall angle (SWA) of 30° with respect to the vertical plane, a period $\Lambda = 515$ nm, a groove depth $\sigma = 102$ nm, and a duty-cycle DC = 49.4% (on top). After deposition of the Ta_2O_5 waveguide layer, the grating profile at the interface between air and waveguide also exhibited a trapezoidal shape, however with a slightly different SWA estimated to be 37.5° with respect to the vertical plane. The period remains unchanged ($\Lambda = 515$ nm), the groove depth and duty-cycle were measured to be $\sigma = 132$ nm and DC = 53% (on top) respectively. A RCWA simulation, making trapezoidal fits to the measured grating profiles at both air -Ta_2O_5 and Ta_2O_5- sapphire interfaces, as depicted in Fig. 3 left, and a

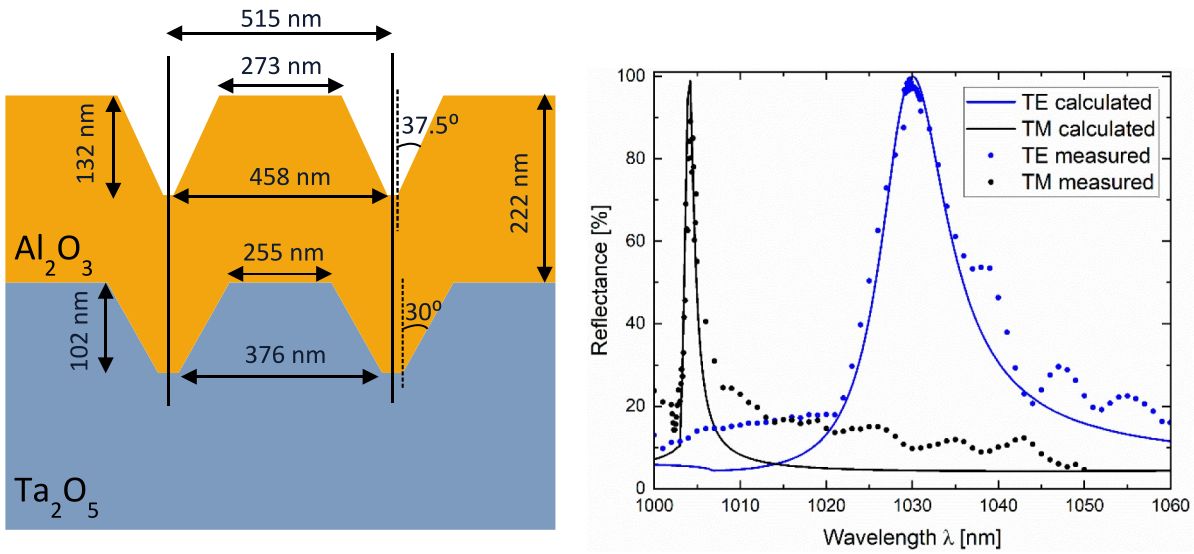

Fig. 3 Left: Approximated grating profiles (revealed by AFM measurements) used for the simulation. Right: Calculated and measured reflectance at an AOI of 11.5°

waveguide-layer thickness of 222 nm (which is close to the nominal value of 230 nm and corroborated by an ellipsometry measurement of a separate witness sample on a silicon substrate giving a deposition thickness of 225 nm). As can be seen in Fig. 3 (right), there is a good agreement between the measured reflectance spectra and the calculated ones, despite the oscillations in the measured values due to the back-surface reflection. Considering an average of the measured groove depth of the RWG, the propagation length, L, of the TE mode was analytically estimated to be ≈13 μm [11]. This value is approximately 3–4 times smaller than what is expected for the propagation length of the TE mode in a single-corrugated RWG with similar grating parameters. This in turn results in an improved thermal behavior, though at the expense of the spectral selectivity [7].

5 Laser performance

After the characterization of the fabricated RWGs as described above, its performance was tested by employing it as a folding mirror in an Yb:YAG TDL resonator. The first experimental setup was designed for multi-mode (MM) operation ($M^2 \approx 6$) using the resonator design depicted in Fig. 4a. This resonator comprised a plane highly reflective (HR) end mirror, the RWG or HR reference mirror as folding mirror, the thin-disk crystal, and a plane output coupler (OC) with a transmission of 8%. The resonators mirrors used in these experiments are standard and commercially available mirrors based on fully dielectric coatings deposited on fused silica substrates.The 130 μm thick-disk, with a doping concentration of about 10–11 at.% ($N_{dop} = (13.8 - 15.1) \times 10^{20} cm^{-3}$) was pumped with a fiber-coupled laser diode delivering a maximum power of 495 W at a wavelength of 940 nm. The thin-disk crystal with a diameter of 12 mm was glued onto a water-cooled diamond heat sink, resulting in a concave radius of curvature (RoC) of 1.7 m. The mounted disk was installed in a pumping module providing 12 reflections (24 passes) of the pump radiation at (through) the laser crystal. The diameter of the pump beam at the disk was set to 3.2 mm. At the maximum pump power density of 6.16 kW/cm^2, the RoC of the disk was estimated to be 1.77 m.

The performance of the TDL oscillator was qualified with a standard HR plane mirror prior to implementing the RWG. The laser performances obtained in both experiments are shown in Fig. 5. An average output power of 267 W was extracted with an optical efficiency of 54%, when the standard HR mirror was used. With the RWG, the maximum output power was reduced to 191 W with a corresponding optical efficiency of 39%. Thus, an efficiency decrease of 15% points was observed, attributable to the double-pass of the RWG and the associated losses due to its reflectance of 99.2% as compared to the 99.95% of the HR mirror, and the imperfect shape of the surface as will be discussed below. It's worth mentioning that a further increase of the output power was limited by the available pump power of the current setup.

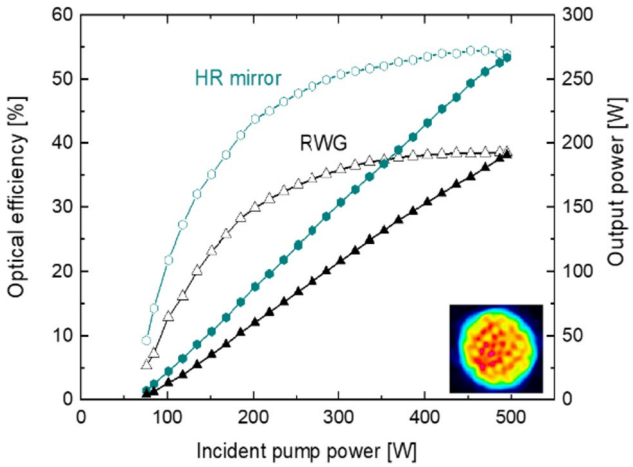

Fig. 5 Laser performance in multi-mode operation. The inset shows the distribution of the intensity at the maximum output power of 191 W, as obtained with the RWG in the resonator. Open symbols: optical efficiency (left ordinate), filled symbols: output power (right ordinate)

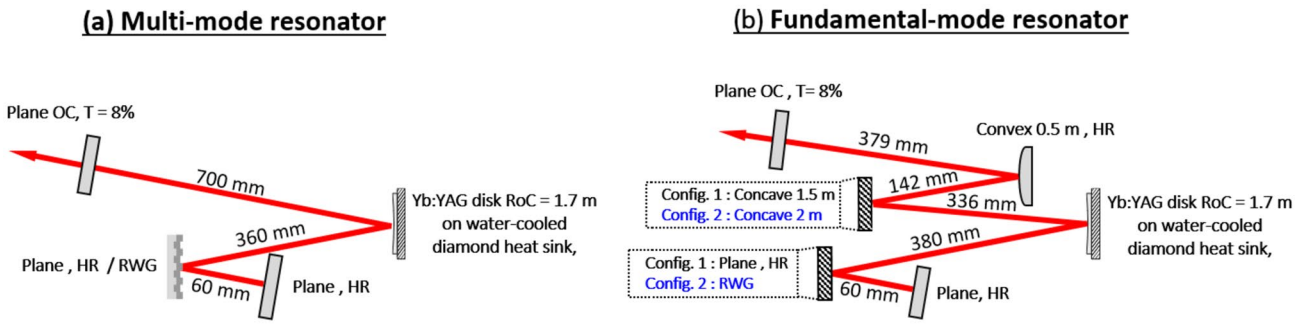

Fig. 4 Design of the **a** Multi-mode ($M^2 \approx 6$) and **b** fundamental-mode Yb:YAG thin-disk laser resonators

The RWG was clamped on a water-cooled holder and the surface temperature of the grating was monitored by means of an Infrared thermal imaging camera (VarioCAM HD Head 980, Jenoptik). A calibration was performed to determine the emissivity of the RWG, which was found to be in the range of 0.71–0.74. The cooling water temperature was set to 19 °C. The rise of the RWG surface temperature as a function of the intra-cavity power density is shown in Fig. 6a. At full pump power the maximum temperature on the surface of the RWG was measured to be 32 °C (corresponding to a temperature rise of only 12 K) at an intra-cavity laser power density on the RWG of 52 kW/cm^2 assuming a beam diameter of 3.36 mm. The linear fit function has a slope of 0.257 K/(kW/cm^2), which corresponds to a reduction by a factor of 46 with respect to the value of 11.86 K/(kW/cm^2) for the RWG on a fused-silica substrate as reported in [6]. The measured spectra of the emitted laser radiations are shown in Fig. 7a. By placing the RWG in the resonator, the spectral bandwidth (recorded with an Optical Spectrum Analyzer Advantest-8384) of the laser emission was reduced from 2.45 nm (with the HR folding mirror) down to 0.5 nm.

A further experiment was devoted to the TDL performance in fundamental-mode operation. Figure 4b illustrates the correspondingly adapted resonator that required two configurations, as will be explained below. A telescope was incorporated to ensure an overlap ratio of $d_M/d_P = 85\%$ between the diameter d_M of the fundamental mode and the diameter d_P of the pump beam on the Yb:YAG disk Fig. 8. The laser performance and the far-field intensity distributions obtained with either the HR mirror or the RWG in the resonators are shown in Fig. 9.

In configuration 1 where the HR folding mirror was implemented, an output power of 122 W was extracted, which corresponds to an optical efficiency of 40.5%. The beam propagation factor was measured to be 1.25. After direct replacement of the HR mirror by the RWG no laser action was obtained without further adjustments, indicating that the 650 µm thick RWG was not ideally plane. An interferometric analysis of the RWG revealed that the surface of the 650 µm thick device appeared to be distorted. The characterization of the form of the RWG by means of a Twyman-Green interferometer revealed a saddle-shape with a peak-to-valley deviation of 63 nm over an aperture of 2.9 mm. Fitting a spherical form to the measured shape corresponds to an estimated concave radius of curvature of about 17 m and required the resonator design to be adapted. The cause of the warped surface of the RWG will need to be established in future investigations. Thin wafers are not typically specified for flatness, however, the surface of the sapphire substrate was not analyzed prior to fabrication of the RWG. There is also the potential that the fabrication processes led to stress-induced deformations. To counter the optical power of the RWG, a slightly adjusted cavity design was set up (configuration 2 in Fig. 4b theoretically providing a similar diameter of the fundamental mode on the disk as for the plane HR mirror. As shown by configuration 1 in Fig. 4b, the plane HR folding mirror was used together with

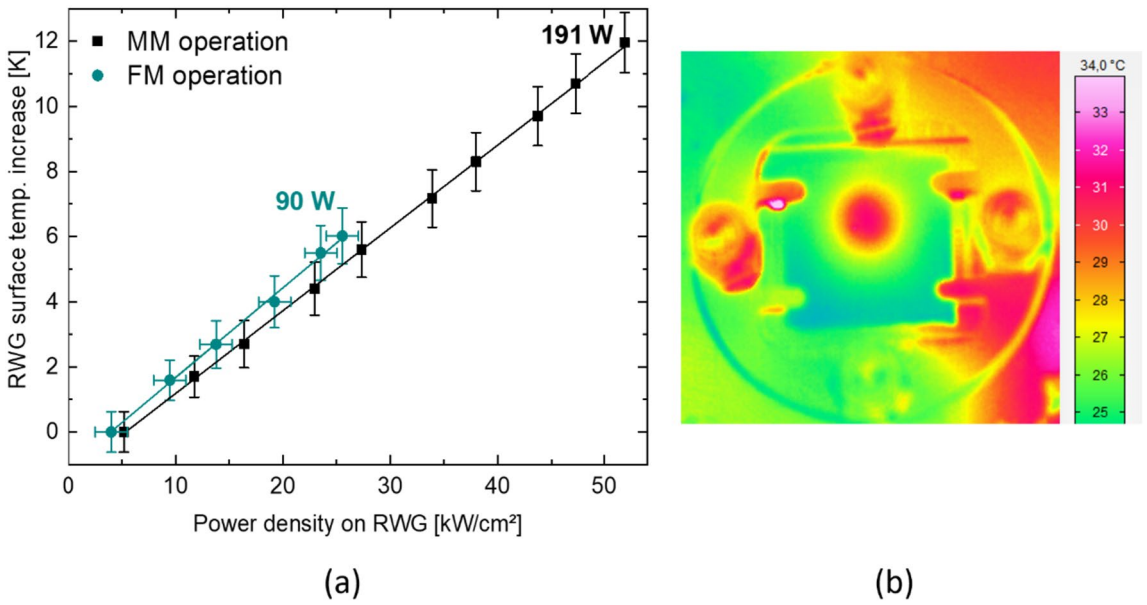

Fig. 6 **a** Rise of the surface temperature of the RWG as a function of the intra-cavity power density in multi-mode (MM) and fundamental-mode (FM) operation. **b** Infrared thermal image of the sample at the maximum output power in multi-mode operation. The error bars were added taking into account the accuracy of the thermal imaging camera as well as that of the estimated beam size ($d \approx 3.3 - 3.4mm$) on the RWG

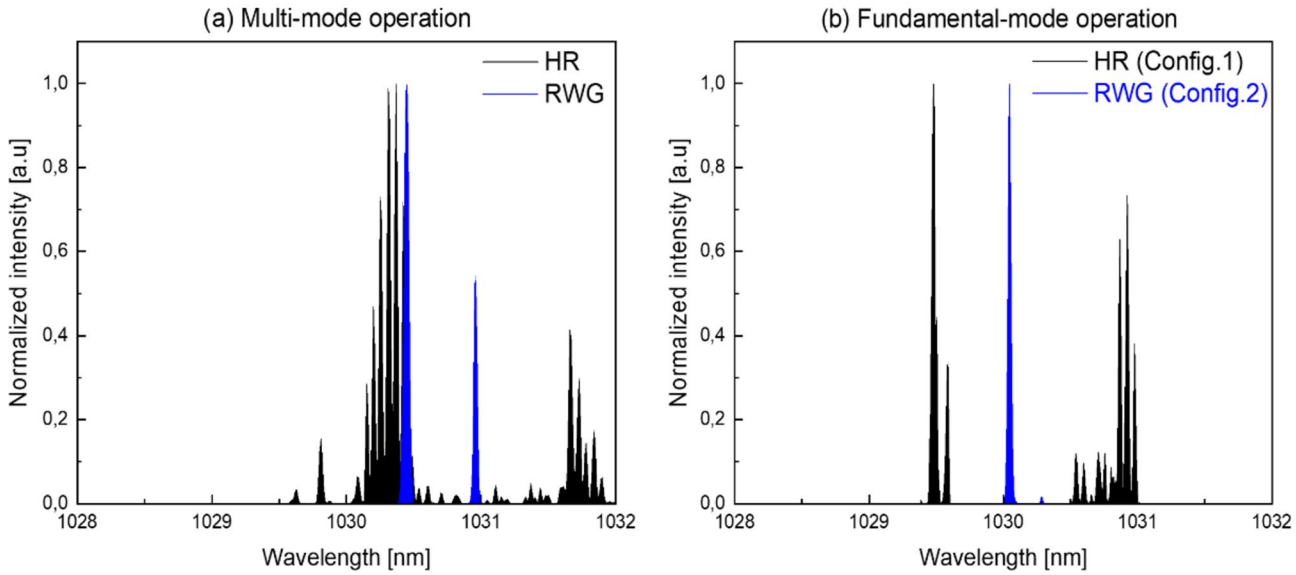

Fig. 7 Recorded emission spectra measured at maximum output power for: **a** Multi-mode operation and **b** Fundamental-mode operation

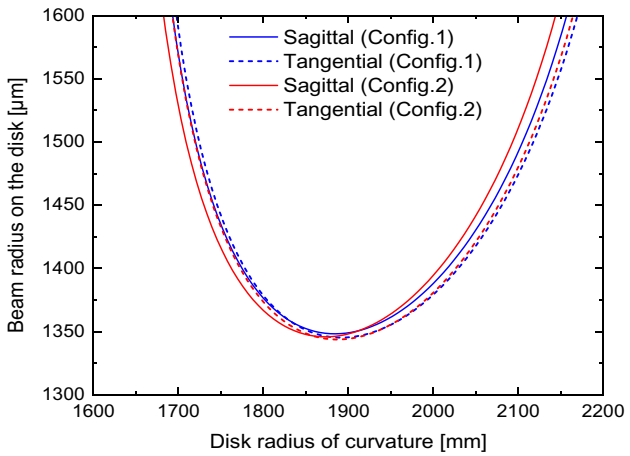

Fig. 8 Calculated radius of the oscillating beam over variation of the radius of curvature of the laser crystal for the two resonator configurations

a concave folding mirror with a RoC of 1.5 m, whereas in configuration 2, when using the RWG, the concave folding mirror was replaced with another with a RoC of 2 m. The calculated mode radii at the location of the thin-disk crystal for the two resonator configurations are shown in Fig. 8, as a function of the power-dependent effective radius of curvature of the thin disk.

In configuration 2, an output power of up to 90 W was achieved at an optical efficiency of 30%. At the maximum output power, the beam propagation factor was measured to be $M^2 = 1.45$. The degradation of the beam quality is mainly attributed to the non-spherical aberrations of the RWG, as determined by the interferometric measurement.

The measured spectra obtained in near fundamental-mode operation are shown in Fig. 7b. The beam generated with the RWG in the resonator exhibited a spectral bandwidth of 28 pm (FWHM), whereas the overall spectral bandwidth was measured to be about 1.6 nm when using the plane HR mirror. The surface temperature on the RWG was measured to be 26 °C (corresponding to a temperature increase of only 6 K) for a power density of 26 kW/cm^2 (see Fig. 6a), with a corresponding slope of 0.277 K/(kW/cm^2). The latter value shows a reduction by a factor of approx. 4 with respect to the slope of 0.99 K/(kW/cm^2) for the multi-corrugated (etched substrate) RWG on a fused-silica substrate reported in [7]. The rate of the increase of the surface temperature with respect to power density for both FM and MM configurations are comparable within the measurements accuracies. For both laser experiments using the RWG, the degree of linear polarization of the emitted laser beam was measured by means of a commercial Stokes-polarimeter to exceed 99%.

6 Conclusion

In conclusion, we have demonstrated for the first time the intra cavity utilization of a resonant waveguide-grating mirror on a sapphire substrate in Yb:YAG thin-disk lasers. The setups were operated with power densities on the RWG equal to 52 kW/cm^2 and 26 kW/cm^2 in multi-mode (output power of 191 W) and fundamental-mode (output power of 90 W) configurations respectively, without any sign of component degradation. The rise of the surface temperature of the RWG was recorded to be less than 12 K and 6 K in both multi-mode and fundamental-mode experiments, respectively.

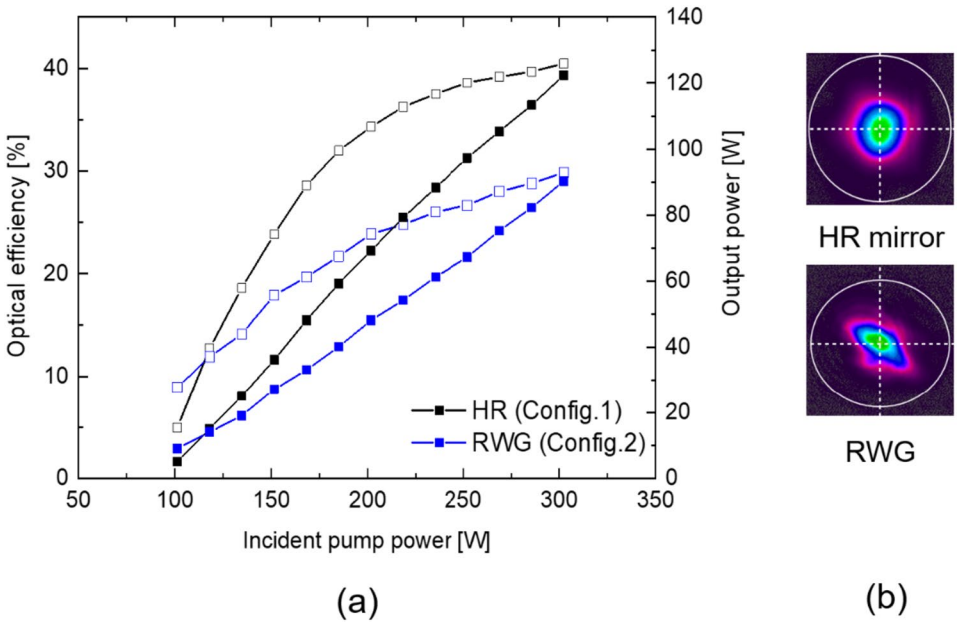

Fig. 9 **a** Power and efficiency curves for fundamental-mode operation. **b** Beam intensity profiles in the far-field with the plane HR and RWG folding mirrors, respectively

These promising results demonstrate that the combination of a sapphire substrate with an optimized RWG design leads to a significant improvement with respect to its power-density handling capabilities, yielding a good laser performance and resilience to the inherent thermal load. Further investigations are presently devoted to improving the fabrication process to produce samples with suitable surface shape, along with an improved reflectance. Further experiments will also be dedicated to the implementation of the sapphire-based RWG in high-power systems to demonstrate the generation of kW-class narrow linewidth, linearly polarized Yb:YAG TDL.

Acknowledgements The authors thank Christof Pruss from the Institut für Technische Optik (ITO) for the support in the wavefronts deformations measurements.

Author contributions DB and AB have contributed equally to this work. MAA and DB provided the design of RWG. AB designed, conducted the laser experiments. DB conducted the spectroscopic characterization of the RWG and participated to the laser experiments. AB and DB formulated the first draft of the manuscript. GM and FL developed the fabrication process of the RWG. PK, MK, JIM,TG and MAA assisted in the preparation of the manuscript. All authors reviewed the manuscript and provided their respectives inputs.

Funding Open Access funding enabled and organized by Projekt DEAL. European Union's Horizon 2020 research and innovation programme under Marie Skłodowska-Curie (813159). JM also acknowledges the U.K. Engineering and Physical Sciences Research Council (EPSRC) for financial support via the grant EP/P027644/1. MK also acknowledges the financial support of the Academy of Finland through the flagship on "Photonics research and innovation" (PREIN, 320166).

Data availability Data underlying the results presented in this paper are not publicly available at this time but may be obtained from the authors upon reasonable request.

Declarations

Conflicts of interest The authors declare no conflicts of interest.

References

1. I.A. Avrutskiĭ Sovn, G.A. Golubenko, V.A. Sychugov, A.V. Tishchenko, Sov. J. Quantum Electron. 1063 (1986)
2. GA Golubenko AS Svakhin VA Sychugov AV Tishchenko 1985 Sov. J. Quantum Electron. 15 7 886 887
3. G Quaranta G Quaranta G Basset OJF Martin B Gallinet 2018 Laser Photonics Rev. 12 1800017
4. R. Magnusson, Kyu J. Lee, Hafez Hemmati, Yeong Hwan Ko, Brett R. Wenner, Jeffery W. Allen, Monica S. Allen, Susanne Gimlin, Debra Wawro Weidanz, Proc. SPIE 10510, Frontiers in Biological Detection:Nanosensors to Systems X (2018)

5. J. Sauvage-Vincent, S. Tonchev, C. Veillas, S. Reynaud, Y. Jourlin, J. Eur. Opt. Soc. **8** (2013)
6. M.M. Vogel, M. Rumpel, B. Weichelt, A. Voss, M. Haefner, C. Pruss, W. Osten, M. Abdou Ahmed, T. Graf, Opt. Express **20**, 4024–4031 (2012)
7. M. Rumpel, B. Dannecker, A. Voss, M. Moeller, C. Moormann, T. Graf, M. Abdou Ahmed, Opt. Lett. **38**, 4766–4769 (2013)
8. A. Aubourg, M. Rumpel, J. Didierjean, N. Aubry, T. Graf, F. Balembois, P. Georges, M. Abdou Ahmed, Opt. Lett. **39**, 466–469 (2014)
9. F. Pigeon, J.C. Pommier, S. Reynaud, O. Parriaux, M. Abdou Ahmed, S. Tonchev, N. Landru, J. P. Fève, Opt. Express **15**, 2573–2584 (2007)
10. T. Dietrich, S.Piehler, M. Rumpel, P. Villeval, D. Lupinski, M. Abdou Ahmed, T. Graf, Opt. Express **25**, 4917- 4925 (2017)
11. VA Sychugov AV Tishchenko NM Lyndin O Parriaux 1997 Sens. Actuators B Chem. 39 1–3 360 364
12. IH Malitson 1962 J. Opt. Soc. Am. 52 1377 1379
13. MG Moharam DA Pommet EB Grann TK Gaylord 1995 J. Opt. Soc. Am. A 12 1077
14. G. Mourkioti, D. Bashir, G.A. Govindassamy, F. Li, R.W. Eason, T. Graf, M. Abdou Ahmed, J.I. Mackenzie, Appl. Phys. **129**, 66 (2023)